



## Protective effect of carvacrol on biochemical, immunological and gill morphological induction through reduced graphene oxide (rGO) exposure on zebrafish (*Danio rerio*)

Bichandarkoil Jayaram Pratima<sup>1</sup>, Ravichandiran Ragunath<sup>1</sup>, Namasivayam Nalini<sup>2\*</sup>

<sup>1</sup> Department of Biochemistry and Biotechnology, Faculty of Science, Annamalai University, Tamil Nadu, India

<sup>2</sup> Professor and Head, Department of Biochemistry and Biotechnology, Faculty of Science, Annamalai University, Tamil Nadu, India

### Abstract

**Background:** Reduced graphene oxide (rGO) is a carbon nanomaterial with specific properties, which allow its use in several areas. Some studies have characterized the effects of rGO on aquatic organisms, but the ability to recover after exposure remains largely unknown.

**Aim:** In the present study, the toxicity of reduced graphene oxide (rGO) was studied in zebrafish (*Danio rerio*) using biomarkers of oxidative and metabolic stress, immunological dysfunction, and cellular damage. The gill tissues were morphologically assessed and also the best dose of carvacrol (CVC) for neutralizing adverse effects was analyzed.

**Methodology:** Fish were fed for fourteen days, and eight study groups were investigated: control, rGO exposure alone (10 mg L<sup>-1</sup>) and combined with three different carvacrol doses (10 mg L<sup>-1</sup> of rGO + carvacrol 100, 150 or 200 mg kg<sup>-1</sup> of food).

**Result:** *D. rerio* exposed to rGO alone or in combination with a lower carvacrol dose demonstrated overall inferior results compared to control groups and those supplemented with rGO and 150 or 200 mg kg<sup>-1</sup> carvacrol. rGO impairs cells by increasing LDH activity and cortisol levels and inducing oxidative stress by reducing SOD and CAT activity and suppressing the immune system through lysozyme activity. Lesions in gill tissues included cells with peripheral nuclei. rGO exposure increased apoptotic and necrotic gill cells. The structural study of the gill tissues revealed multiple lesions, including a dilated marginal channel, lamellar fusion, clubbed tips, swelling mucocytes, epithelial lifting, aneurysms and necrosis.

**Conclusion:** As a result of our findings, we believe that a sub-lethal dosage of rGO could be hazardous to fish species, posing a threat to the aquatic food chain. Although rGO is harmful to the groups exposed to it, CVC supplementation at 150 or 200 mg kg<sup>-1</sup> can protect against its toxic effects.

**Keywords:** carvacrol, carbon nanomaterial, nanoparticle, metabolic stress, oxidative stress, zebrafish

### Introduction

Graphene, a one-atom-thick monolayer of sp<sup>2</sup> bonded carbon atoms organized in a two-dimensional honeycomb structure, has recently received significant attention in several disciplines of nanotechnology study [1]. Reduced graphene oxide (rGO) is one of the most commonly synthesized carbon nanomaterials in large quantities [2]. Because of their distinct and desired properties, nanomaterials such as rGO have seen tremendous growth in the domains of transistors, chemical sensors, biosensors and organic solar cells [3-5]. As nanoparticles are increasingly used in everyday products like pharmaceuticals, biomedical, cosmetic, and sporting goods, they are inevitably dispersed into the environment via air, water, and soil. So, in addition to the benefits of employing nanomaterials, raising public awareness about their toxicity is vital to prevent adverse environmental repercussions. [6-7]. In addition to the immediate consequences, the potential toxicity of nanomaterials to the environment is unknown, and it should be closely monitored. As a result, the investigation to establish nanotoxicity is critical and has considerable scientific, social, and economic value [8]. Some studies in recent years have focused on the toxicity of metallic nanoparticles, semiconductor quantum dots, carbon compounds, and other materials [9-12]. The environmental dangers of the innovative carbon nanomaterials, on the other

hand, are still unknown. Surface properties, structural traits, and nanoparticle aggregation in the real world may alter their toxicity [13].

A few research in recent years has reported on the environmental implications of carbon nanoparticles. Zhang *et al.* published research on the toxicological effects of carbon nanomaterials on several cell types [14-20]. Zhu *et al.* observed that Buckminsterfullerene (C<sub>60</sub>) aggregation reduced zebrafish survival and hatching rates [21]. Zhang *et al.* and Liu *et al.* investigated the impact of graphene and rGO on human health [22, 23]. Akhavan *et al.* studied the antibacterial toxicity of graphene and rGO [24]. These carbon nanoparticles impact human health, plants, and animals, among other things. The toxicity of rGO in aquatic environments, on the other hand, is unknown.

*Danio rerio* was chosen for this study because it is a standardized organism frequently used in scientific research due to its unique characteristics, including ease of laboratory care, rapid development, small size, low cost, and near resemblance to the human genome [25-27]. Additionally, this species has been used as a standard for determining the toxicity of various NPs by examining biochemical, molecular, and behavioural responses [27, 28]. While multiple studies have been conducted on the toxicity of graphene oxide to aquatic species, few have examined their ability to recover following post-exposure periods in the absence of

NPs. Metabolic imbalances generated by nanoparticle exposure may persist even after the stressor has been eliminated, resulting in severe consequences for individuals and groups. Recovery evaluation is critical for aquatic biota conservation efforts in particular.

Carvacrol (CVC:  $C_{10}H_{14}O$ ) is a liquid phenolic monoterpenoid found in the essential oils of oregano (*Origanum vulgare*), thyme (*Thymus vulgaris*), pepperwort (*Lepidium flavum*), and wild bergamot (*Citrus aurantium var. bergamia Loisel*), among others [29]. Commercial CVC is manufactured using chemical and biotechnological techniques [30]. Carvacrol is a lipophilic compound with a density of 0.976 g/ml at 25 °C: it is insoluble in water but soluble in ethanol, acetone, and diethyl ether [31]. As recently reviewed by multiple authors, this molecule exhibits a broad range of biological activities, including antibacterial and antifungal, antiviral, antioxidant, and anticarcinogenic properties [32-37]. Due to its flavour and antimicrobial capabilities, CVC has been considered a natural food preservative in the food industry [38, 39]. Additionally, CVC is a significant component of plant extracts derived from *Zataria multiflora Boiss*, *Satureja hortensis*, and *Oryza vulgare*, mediating the antibacterial, antioxidant, anti-inflammatory and anti-cancer actions of these plants [40-42].

Many indicators are employed in ecotoxicology to measure exposure to environmental pollutants [43,44]. These biomarkers provide crucial insight and correlation into the harmful effects of xenobiotics on the organisms that have been exposed to them. The primary goal of this study was to determine the optimal dose of carvacrol (CVC) to reverse the damage caused by rGO NPs exposure in the zebrafish (*Danio rerio*), which is a well-characterized vertebrate model for toxicity assessment. The study employed a multi-biomarker and morphological approach to determine the optimal dose of carvacrol and reverse the damage caused by rGO NPs exposure in the zebrafish.

## Methodology

### Reduced Graphene oxide (rGO) synthesis and characterization

Hummer's technique was used to produce graphene oxide [45]. This was done by mixing 1 g of natural graphite powder in an ice bath while keeping the temperature below 20°C. Then, while stirring, 6 g  $KMnO_4$  was added gradually. This was followed by another 15 minutes of agitation with 70 ml water after which 80 ml of 30%  $H_2O_2$  solution was added to the residual  $KMnO_4$  until no more bubbles appeared and the reaction was complete. Finally, the obtained product was rinsed several times to remove any salt residue. rGO black powder was obtained after three hours of thermal reduction at 200°C. The synthesized rGO was characterized by UV-Vis absorption spectroscopy, FTIR spectroscopy, X-Ray Diffraction Spectrometry and SEM.

### Fish and experimental conditions

We obtained 80 zebrafish (*Danio rerio*) weighing  $1.93 \pm 0.2$ g from a local fish market in Kolathur, Chennai, Tamil Nadu. Before the trial, fish were acclimatized for one week and fed commercial meals three times daily. The photoperiod was maintained at 12L:12D, and the water temperature was kept constant at  $(26.0 \pm 1.0^\circ C)$ . Daily measurements were taken for the following water physicochemical parameters: pH and dissolved oxygen levels. Eight test groups were used in the experiment, namely:

- 0+0 - fish fed the control diet:
- 0+10 - fish fed the control diet+10 mg  $L^{-1}$  of rGO:
- 100+0 - fish fed the control diet+ carvacrol (100 mg  $kg^{-1}$  of food)
- 100+10 - fish fed the control diet+ carvacrol (100 mg  $kg^{-1}$  of food) + 10 mg  $L^{-1}$  of rGO:
- 150+0 - fish fed the control diet + carvacrol (150 mg  $kg^{-1}$  of food):
- 150+10 - fish fed the control diet+ carvacrol (150 mg  $kg^{-1}$  of food) +10 mg  $L^{-1}$  of rGO:
- 200+0 - fish fed the control diet + carvacrol (200 mg  $kg^{-1}$  of food):
- 200+10 - fish fed the control diet+ carvacrol (200 mg  $kg^{-1}$  of food) +10 mg  $L^{-1}$  of rGO

In 30 L aquariums, fish were randomly distributed. For 14 days, fish were fed twice a day, at 10:00 a.m. and 15:00 p.m. Sampling took place 14 days following exposure.

### Food preparation and sampling

Dietary requirements for all groups were identical: 51.1% crude protein, 13.6% lipids, 10.2% ash, and 3.55% fiber. rGO dosages (10 mg  $L^{-1}$ ) and three dosages of carvacrol were given to the diet (100, 150, or 200 mg  $kg^{-1}$  of food). All fish blood was collected from their caudal veins and allowed to clot for 2 hours at room temperature. They were then centrifuged at 3000 rpm for 15 minutes at 4°C. A serum pool was preserved at -80°C for immunological and enzymatic tests [46].

### Biomarkers of immune, oxidative, and metabolic stress

The serum lysozyme activity was determined by combining 50  $\mu L$  of *D. rerio* serum with 2 mL of a *Micrococcus lysodeikticus* solution (0.2 mg  $mL^{-1}$ ) in a 0.05M sodium phosphate buffer (pH 6.2). The reaction was carried out at room temperature and spectrophotometric absorbances at 450 nm were measured after 5 minutes.

The activity of superoxide dismutase (SOD) and catalase (CAT) was evaluated by measuring the decrease in absorbance at 240 nm with 50mM  $H_2O_2$  as the substrate [47, 48]. In addition, serum lactate dehydrogenase (LDH), alkaline phosphatase (ALP), alanine aminotransferase (ALT), acid phosphatase (ACP) and aspartate aminotransferase (AST) activities were analyzed and evaluated in serum using [49].

Commercial kits measure glucose, cortisol, total protein, albumin, and globulin (Sigma Aldrich, India). Assays for cortisol and glucose were performed according to the protocol reported in Shaluei *et al.* 2012 [50]. Next, the total protein content was measured using the method described by Bradford *et al.* 1976 [51], with bovine serum albumin serving as a reference. The acidic pH test employed a bromocresol green reagent to measure serum albumin levels. Finally, we got serum globulin concentrations by subtracting albumin from total serum protein concentrations [52].

### Histological examination

After 14 days, the gill samples were preserved in buffered formalin, embedded in low melting point paraffin (56°C) and sectioned (5.0 mm). They were dehydrated in ethanol for many hours after washing twice in 10 mM PBS. The tissue was stained with H&E and examined under a light microscope (Nikon Eclipse 50i).

### Statistical analysis

The mean  $\pm$  SEM was used to represent all the data. Comparing the outcomes of the different groups was done using a one-way analysis of variance followed by a DMRT test for comparisons between the groups. A p-value of less than 0.05 was considered statistically significant in all groups.

### Results

#### Characterization of rGO

##### UV-Vis spectroscopy

Ultraviolet-visible spectroscopy was used to monitor the degree of oxidation of rGO. rGO spectrum produced is illustrated in Fig 1. The absorption peak was discovered at 230 nm.

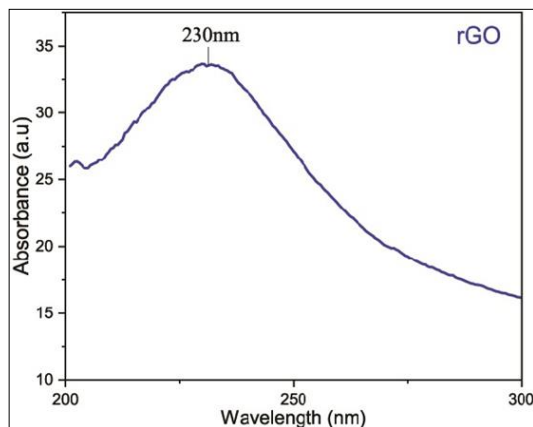


Fig 1: UV-Visible spectrum of rGO

##### X-Ray diffraction (XRD)

The crystal phase and interlayer spacing of rGO were investigated using XRD. Fig 2 depicts the rGO XRD spectra. After the oxygen-containing functional groups were considerably removed during the thermal reduction, a more prominent peak for rGO was detected at  $2\theta = 26.5^\circ$ . The creation of single layers of rGO could explain the poor organization. The calculated crystal size was in the 12.4nm range.

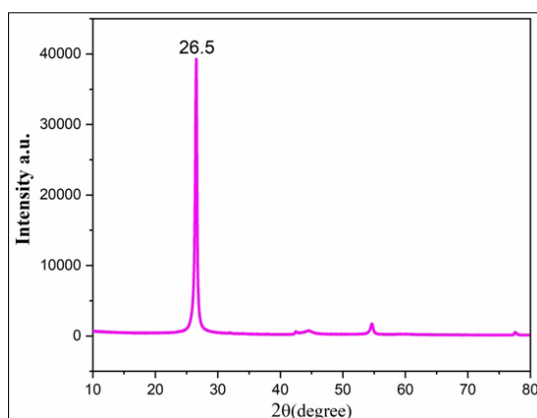


Fig 2: X-ray diffraction spectrum of rGO

##### Fourier transform infrared spectroscopy (FTIR)

The FTIR spectra of rGO are shown in Fig 3. The Fourier transform infrared spectroscopy was used to determine the existence of functional groups in the samples based on their vibrational (transmittance/absorption) spectra. According to

this method, the absorption of infrared light energy with wavelengths ranging from 4000 to 400  $\text{cm}^{-1}$  causes the vibrational excitation of molecular bonds. When the quantity of oxygen-containing functional groups in rGO is reduced, it is expected to have a limited number. The peak value for rGO was  $3401 \text{ cm}^{-1}$  (O-H stretching). Also noticeable are the other peaks at  $1697 \text{ cm}^{-1}$  (C=O vibration),  $1397 \text{ cm}^{-1}$  (O-H deformation),  $2982 \text{ cm}^{-1}$  (C-H stretching vibration) and  $857 \text{ cm}^{-1}$  (-CH bend) in rGO's FTIR spectrum. The spectrum became less, which may also be due to the removal of oxygen during the thermal reduction process. Consequently, the oxygen-containing functional groups were partially eliminated, with only trace amounts of functional group residue remaining at the rGO's edge and basal plane, where they were initially present.

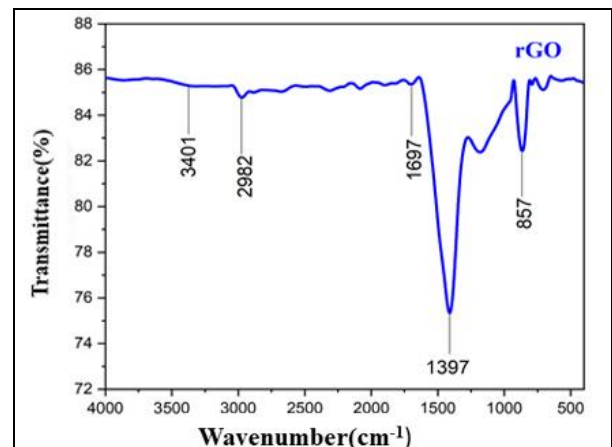


Fig 3: FTIR spectra of rGO

##### SEM and EDX

The morphologies of rGO samples were examined using the SEM technique. The surface of the material was significantly magnified in the micrographs produced by scanning electron microscopy (SEM). Fig 4 shows greater magnification micrographs of rGO samples taken at different magnifications.

The synthesized rGO had a uniform shape and a smooth surface, and this surface demonstrated the sinuate structural characterization of rGO. rGO may have depleted oxygen-containing functional groups as a result of their removal. Table 1 represents the EDX analysis showing firm carbon peaks, consistent with the high percentage of carbon in rGO,

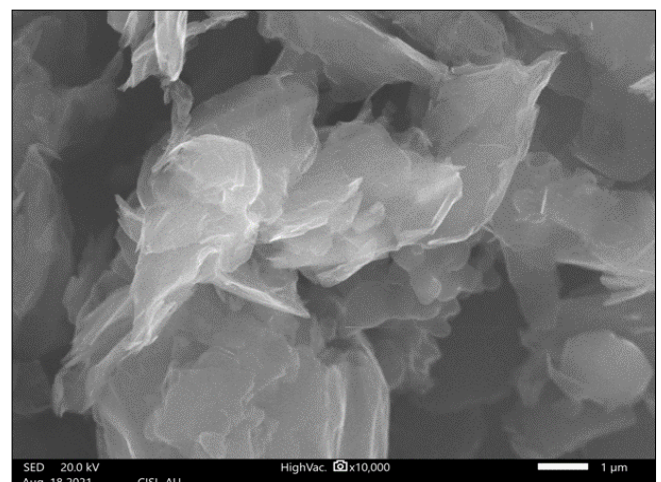
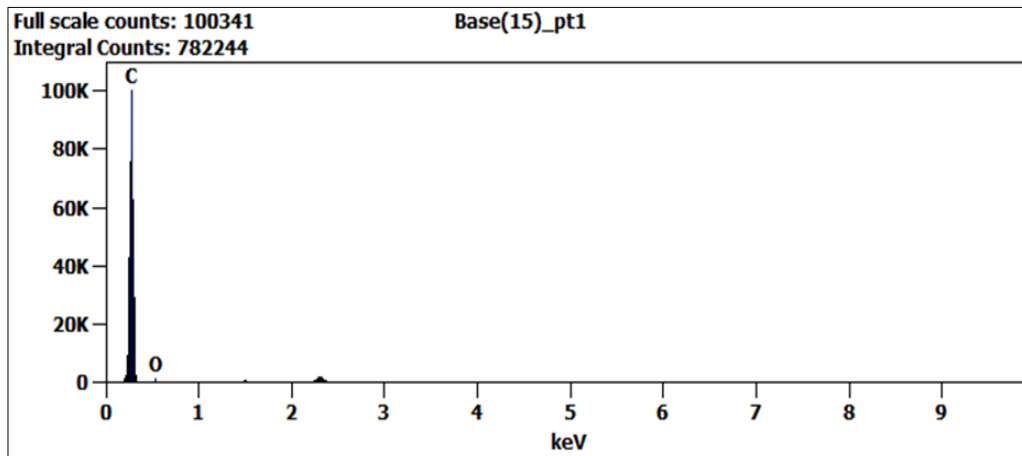


Fig 4: SEM for rGO

**Table 1:** EDX measurements of rGO

Elements	Mass%	Atom%
C	85.06±0.37	88.35±0.39
O	14.94±0.23	11.65±0.18

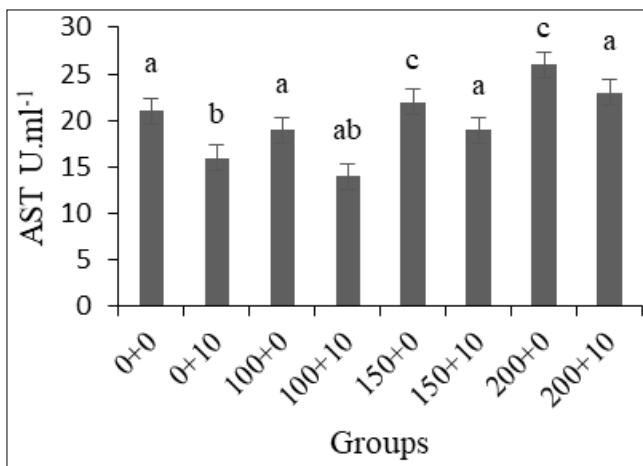


**Fig 5:** Energy-dispersive X-ray for rGO

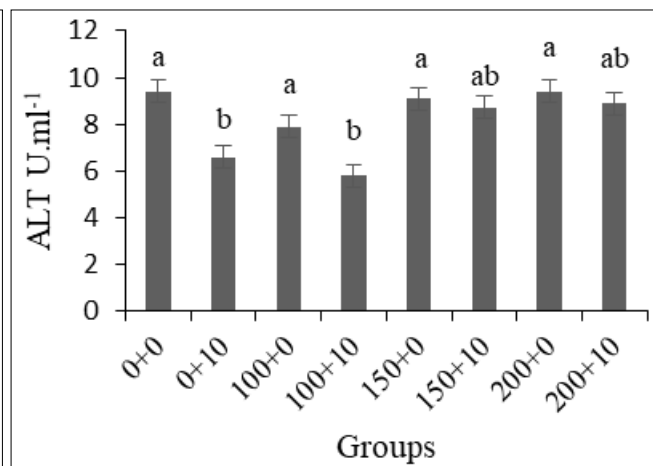
**Levels of immunological, oxidative stress and metabolic stress biomarkers**

When the 0+10 and 100+10 groups were compared to the control, the serum enzymes AST, ALT, ACP and ALP activity was significantly reduced in the 100+10 group (Fig. 6a, 6b, 6c and 6d). Comparisons were made between groups treated with rGO and 150 or 200 mg kg<sup>-1</sup> of carvacrol or with rGO alone, whereas groups not treated with either carvacrol or rGO revealed no differences in inactivity. Compared to the other groups, the groups treated with rGO alone and rGO paired with the lowest carvacrol dose had significantly higher LDH activity (Fig. 6e). When comparing the 0+10, 0+150, 10+150, and 0+200 groups to the control and 0+100, 10+100, and 10+200 groups, the 0+10, 0+150, 10+150, and 0+200 groups had higher glucose levels (Fig. 6f). Cortisol levels were significantly higher in all groups treated with rGO compared to the control group or those exposed to both rGO and carvacrol (Fig. 6g). On the other hand, the group exposed to the rGO had much

greater cortisol levels than those exposed to the rGO and carvacrol. SOD and CAT activity were significantly reduced in the groups exposed to rGO alone, and rGO combined with the lowest carvacrol dose (Fig. 7a and 7b) compared to the other groups and the control, respectively. When the 10+0 and 10+100 groups were compared to the different experimental groups, it was discovered that the serum biochemical markers total protein and albumin were lower in the 10+0 and 10+100 groups. On the other hand, the groups that received 150 mg kg<sup>-1</sup> and 200 mg kg<sup>-1</sup> of carvacrol had significantly greater total protein and albumin (Fig. 8a and 8b). In addition, the lysozyme activity and globulin levels in the humoral innate immune system were significantly higher in the group supplemented with the highest dose of carvacrol than in any of the other groups in the current investigation (Fig. 8c and 8d). The groups exposed to the rGO alone or combined with the lowest dose of carvacrol supplementation had decreased lysozyme activity (Fig. 8d).



a



b

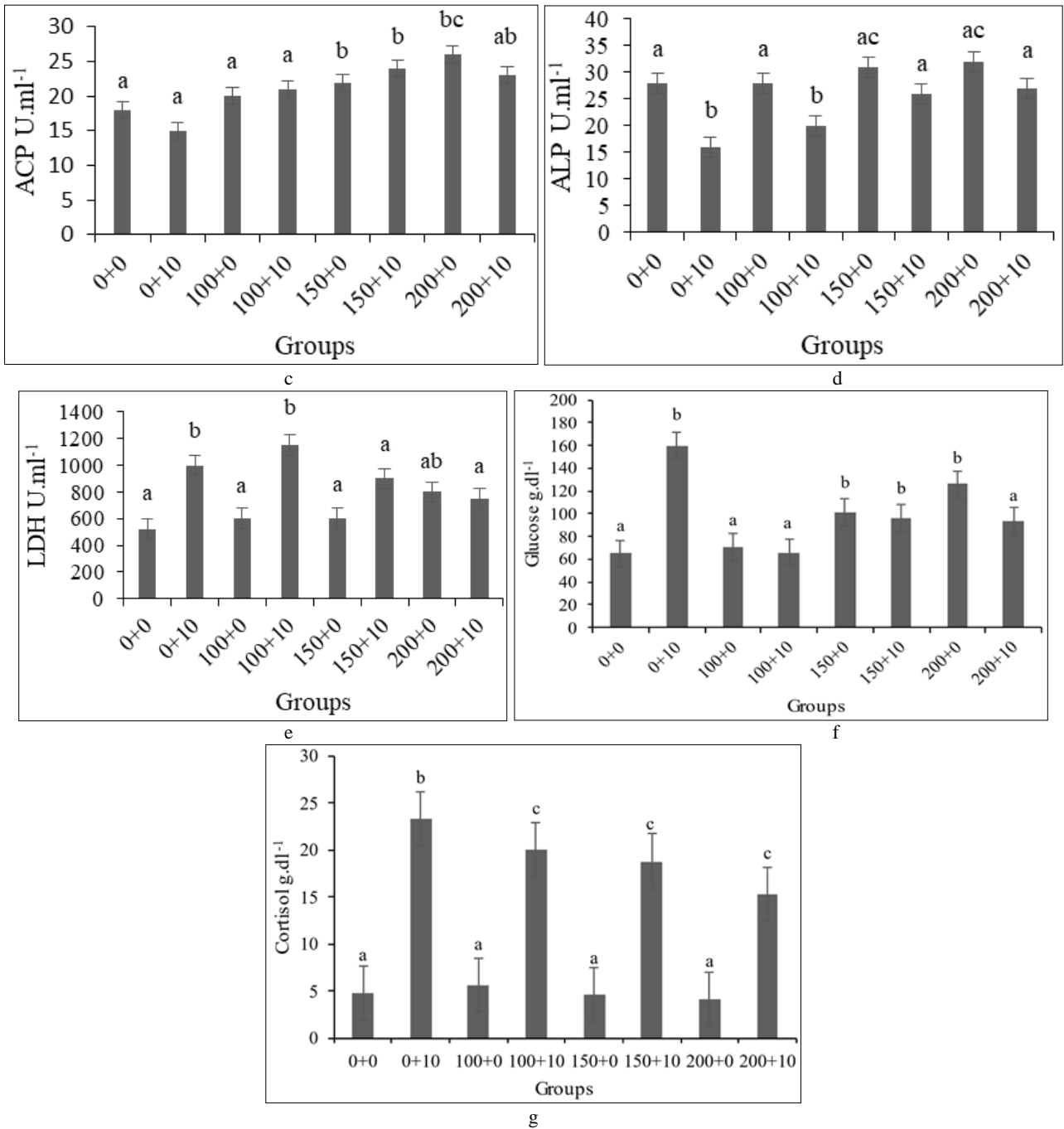


**Fig 6:** Biochemical markers in the serum of *Danio rerio* indicating cellular damage

(a) AST (U.ml<sup>-1</sup>): b) ALT(U.ml<sup>-1</sup>): c) ACP (U.ml<sup>-1</sup>): d) ALP (U.ml<sup>-1</sup>): e) LDH (U.ml<sup>-1</sup>): f) Glucose (g.dl<sup>-1</sup>): g) Cortisol (g.dl<sup>-1</sup>). 0+0, 0+10, 100+0, 100+10, 150+0, 150+10, 200+0,

200+10 indicate the test groups. Data are expressed as mean± standard error of means. Different letters indicate the significant differences between the groups (p < 0.05).

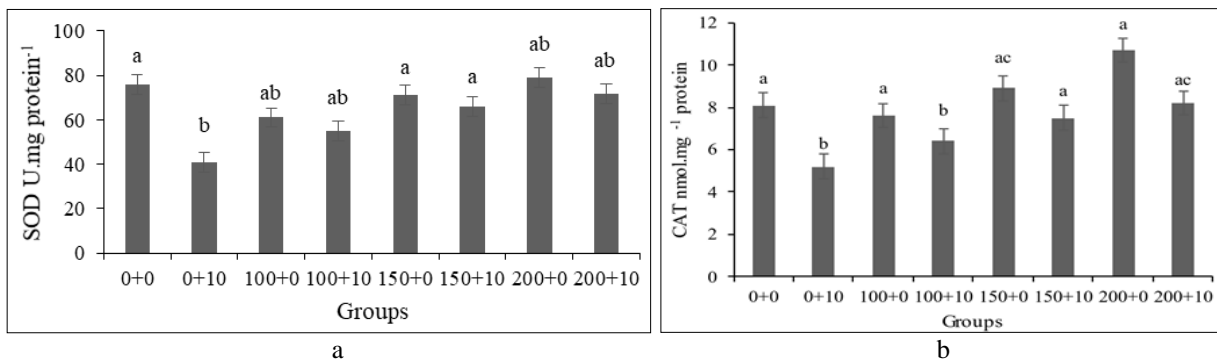


**Fig 7:** Oxidative stress biomarkers in *Danio rerio* serum

(a) SOD activity ( $\text{U} \cdot \text{mg} \text{prot}^{-1}$ ): b) CAT activity ( $\text{nmol} \cdot \text{mg}^{-1} \text{prot}$ ). 0+0, 0+10, 100+0, 100+10, 150+0, 150+10, 200+0, 200+10 indicate the test groups. Data are expressed as

mean  $\pm$  standard error of means. Different letters indicate the significant differences between the groups ( $p < 0.05$ ).

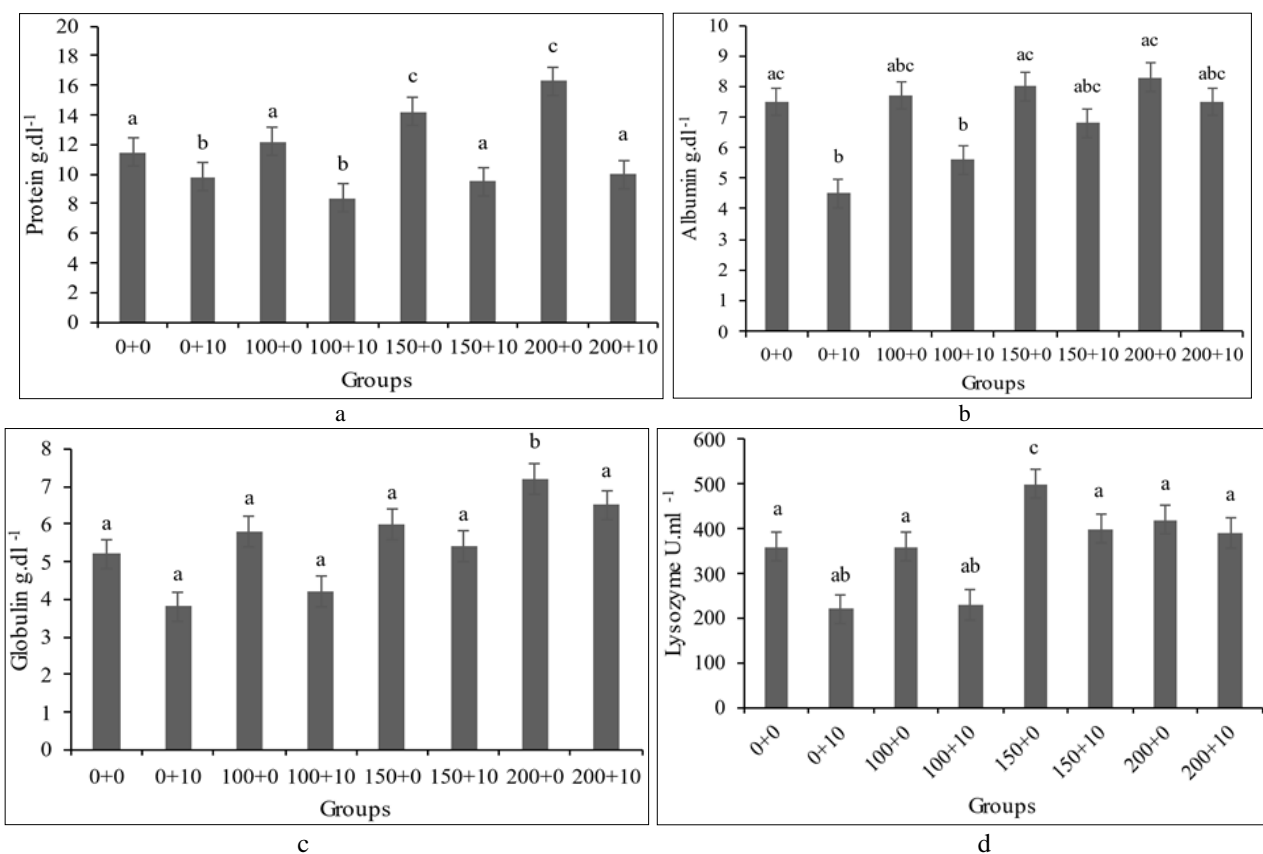


Fig 8: Immunological response biomarkers in *Danio rerio* serum

(a) Protein levels ( $\text{g} \cdot \text{dl}^{-1}$ ): b) Albumin levels ( $\text{g} \cdot \text{dl}^{-1}$ ): c) Globulin levels ( $\text{g} \cdot \text{dl}^{-1}$ ): d) Lysozyme activity ( $\text{U} \cdot \text{ml}^{-1}$ ). 0+0, 0+10, 100+0, 100+10, 150+0, 150+10, 200+0, 200+10 indicate the test groups. Data are expressed as mean  $\pm$  standard error of means. Different letters indicate the significant differences between the groups ( $p < 0.05$ ).

lamellae or filaments emerge is responsible for the gill arch, covered with epidermal tissue specific to the organism. Some histological abnormalities were found in the tissues of fish exposed to the rGO. In the gills of the fish exposed to 10 mg L<sup>-1</sup> rGO for an extended period, the dilated marginal channels were accompanied by lamellar fusion and clubbed tips, aneurysm formation and necrosis in the gills. After treatment with carvacrol, swollen mucocytes, epithelial lifting, aneurysms, and necrosis were reduced, showing that the groups treated with carvacrol after continuous exposure to rGO had less harm.

**Prolonged exposure and histopathology examinations**

As illustrated in Fig.9 (a-h), the morphological structure of the gills in the control group appeared to be expected. A curved structure from which double rows of paired primary

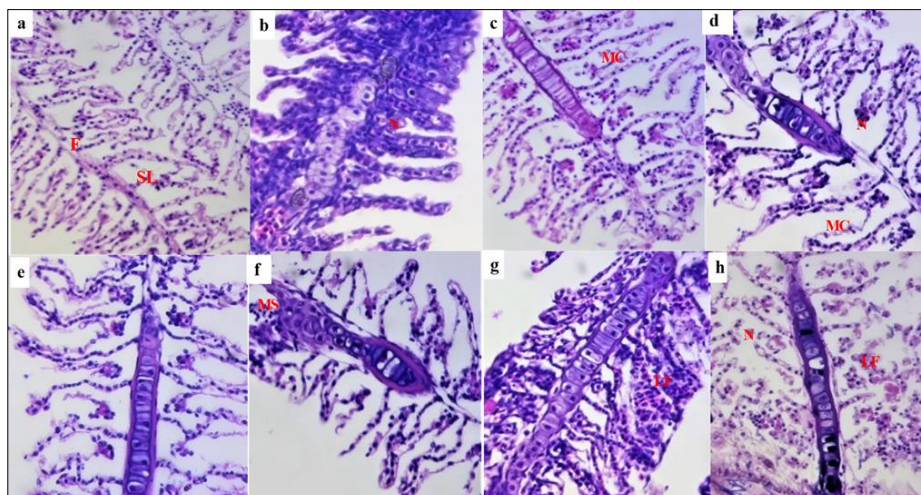


Fig 9: Gill morphology of the adult zebrafish (*Danio rerio*) following exposure to rGO for 14 days.

(a) control group exhibiting normal histology, including a gill arch formed by filaments (F) and secondary lamellae (SL); (b) cells exposed to 10 mg L<sup>-1</sup> rGO exhibited necrosis (N) (c, e and g) cells exposed to 100 mg kg<sup>-1</sup>, 150 mg kg<sup>-1</sup> and 200 mg kg<sup>-1</sup> exhibited dilated marginal channel (MC) and lamellar fusion (LF) (d, f and h) fish exposed to rGO. Different doses of carvacrol revealed necrosis (N), dilated marginal channel (MC), lamellar fusion (LF) and epithelial lifting (EL).

## Discussion

The unique features of rGO indicate that it is well suited for a wide range of applications, including solar cells, aircraft, biosensing, illness diagnosis and antiviral materials. Compared to GO, rGO demonstrates more vigorous activity, improved biocompatibility, better dispersion, and more binding sites due to its structural changes [52-56]. However, due to the widespread usage and manufacture of these nanoparticles, the quantities of these nanoparticles in the environment are increasing over time. rGO and GO are the most extensively used and produced nanoparticles. It is, therefore, impossible to overlook the potential environmental threat that rGO poses. As a result, the present work investigated the possible ameliorative effects of carvacrol against rGO-induced toxicity in zebrafish. To determine the toxicity, rGO was administered to zebrafish for 14 days while being exposed to various concentrations of carvacrol. After the study period, the fish were subjected to multiple biochemical, immunological, and histological examinations.

The liver comprises AST, ALT, ALP, ACP, and LDH [57]. The release of these enzymes into the bloodstream occurs due to damage to hepatic tissues, increasing the activity of these enzymes in plasma [58, 59]. On the other hand, the study results show that the enzymes AST, ALT, ALP, and ACP decrease in groups exposed to rGO combined with a higher carvacrol dose. Rats exposed to rGO have shown similar findings to those described in humans [60]. Inactivation of thiol (-SH) groups aminotransferases by rGO may be the reason for this drop, resulting in the malfunctioning of various processes [51, 52].

When ALT, AST, ALP, and ACP activities were reduced, LDH activity increased in the same groups [43, 44]. Due to the requirement of LDH for pyruvate to lactate interconversion during glycolysis, rGO exposure may alter energy production and cellular metabolic pathways [35]. A relationship between changes in LDH and stress reactions was noticed when rGO was fed to all zebrafish groups. The well-known stress hormone cortisol has increased energy availability through gluconeogenesis, demonstrating that cellular metabolism has been inhibited from synthesizing energy [26]. Increased plasma cortisol levels have been evident in various studies [44, 47]. When metal ions are released from nanoparticles, the generation of ROS increases, resulting in oxidative damage, which includes lipid peroxidation, membrane permeability alterations, protein carbonylation, and DNA damage [58, 49]. SOD is the first enzyme to deal with oxygen radicals, and CAT aids in converting hydrogen peroxide into the water: it is expected that the activity of SOD and CAT will be affected by oxidative stress [39]. Accordingly, we discovered that rGO alone and RGO combined with a lesser quantity of carvacrol supplementation decreased SOD and CAT activity in the groups exposed. There has been some overlap between these

and the findings of [28]. Oxyradicals may accumulate if SOD and CAT activity are inhibited, and oxidative damage will develop. This would indicate that the body's antioxidant defense mechanism has failed to protect it from the harms caused by nanoparticle exposure.

Total protein levels in plasma are employed as a sensitive fish health indicator because high total protein levels suggest liver health problems [20, 29]. As previously reported, rGO-treated zebrafish were shown to have reduced total serum protein and albumin levels and impaired liver function and overall metabolic abnormalities [25]. This study also reveals alterations in protein synthesis due to damage to protein-producing subcellular structures and decreased liver protein production [50]. Apart from that, rGO is hypothesized to lower the production of total proteins and albumin in the liver. Several additional authors have reported that fish exposed to pollution had lower total protein and albumin levels [58].

Researchers assessed the fish innate immunological humoral response parameters by analyzing total serum proteins with cortisol levels [17, 28]. Therefore, it is possible that a slowing of the natural immune response is responsible for the drop in serum proteins and increased plasma cortisol levels reported in fish exposed to rGO in this study. Furthermore, a recent study indicated that fish exposed to GO alone had lower lysozyme activity. Lysozymes demonstrate antibacterial and antiviral action and are essential for the innate immune system [41-43]. As previously reported, this is consistent with previous findings and lends more support to the concept that rGO may be responsible for immunosuppression [34]. According to the results of the biomarkers LDH, CAT, SOD and protein levels in the simultaneous treatments combining rGO and carvacrol, it was discovered that the groups that received 150 mg kg<sup>-1</sup> and 200 mg kg<sup>-1</sup> carvacrol supplementation experienced significant protection against metabolic and oxidative stress, as well as against immune suppression. [55, 56] Because of carvacrol scavenging property, the reduction in ROS occurred via restoration in SOD and CAT activity [44].

Because of the oxidative stress caused by rGO interactions with cell membranes, it is hypothesized that the frequency of zebrafish gill cells experiencing apoptosis and necrosis will be higher than previously observed [36]. In most cases, the production of reactive oxygen species is the primary mechanism of nanoparticle toxicity. According to the previous findings, oxidative stress responses were observed in zebrafish after exposure to GO, including an increase in superoxide dismutase and catalase activity in liver tissues and an increase in glutathione content after GO exposure of [37]. This led them to hypothesize that mitochondria were the principal source of apoptotic responses produced by DNA damage caused by ROS [38, 39]. Another *in vivo* experiment found apoptotic cells in the pachytene region of the gonads of the nematode *Caenorhabditis elegans* after exposure to 10 mg L<sup>-1</sup> GO [50]. This resulted in a loss in the animal's reproductive ability. There are two methods through which rGO may interact with aquatic organisms at the cellular level, both resulting in the generation of oxidative stress. The first is direct penetration, and the second is endocytosis. As a result of biological membrane breakdown, direct penetration of rGO into cells may occur, making its entry into cells more accessible and convenient. Toxins can cause cytotoxicity by inhibiting ion and gas exchanges and blocking nutrition intake by coating cell membranes [41].

As a result of the exposure to reduced graphene oxide, the zebrafish gill cells had a changed appearance. The organism's defense mechanism changes keep rGO from reaching the sensitive gill epithelium previously discovered [32]. However, necrotic cells have been observed in the gill tissues of zebrafish that have been subjected to lower doses (i.e., 100 mg kg<sup>-1</sup>), which may imply that organ function has been impaired. According to the literature, injury to the gill tissues has been observed in the presence of different carbon nanoparticles. For example, it was shown that single-walled carbon nanotubes (SWCNT) could produce lesions on the gills of zebrafish after an acute exposure due to physical irritation and tissue obstruction on the surface of the gills [43]. In addition, researchers discovered that *rainbow trout* developed disorders such as edema, altered mucocytes and hyperplasia [24].

Furthermore, studies confirmed that exposure to fullerene (C<sub>60</sub>) resulted in severe degenerative changes and necrosis in the gill tissue of the *Mussel mytilus sp* [25]. Our study discovered that rGO appeared to accumulate on gill cells, potentially causing harm. Gills are responsible for gas exchange, carbon dioxide emission, and salt and water exchange between the ocean and the atmosphere. These organisms also play a considerable role in the excretion of nitrogenous waste products, especially ammonia. In addition to osmotic dysregulation and respiratory difficulties, the fish is more sensitive to rGO because of the structural damage induced. To provide adequate protection against oxidative stress, antioxidant defenses frequently coordinate. However, it is necessary to provide the proper environmental circumstances for restoring physiological parameters.

Organisms cannot recuperate when stress events linger for an extended period or high-stress levels. Therefore, it is vitally important to create a cause-and-effect link to assess immune responses to the antioxidants properly. In addition, it is important to note that various endpoints in ecotoxicology, including histological, molecular and ROS generation parameters, should be evaluated regularly.

### Conclusion

According to this study, rGO at sublethal doses of 10 mg L<sup>-1</sup> induced oxidative stress, metabolic aberrations, and immune responses in zebrafish: all of these were detrimental. Over time, the gills underwent significant change, which confirmed the rGO organ-specific effects on these tissues during the experiment. On the other hand, supplementation with carvacrol at a higher dose was protective against rGO exposure.

The most beneficial amount of carvacrol supplementation for mitigating the harmful effects of rGO exposure was between 150 and 200 mg kg<sup>-1</sup>. When it comes to determining the potential of organisms to recover after protracted exposure periods, evidence is scarce in the literature. As a result of the findings of this study, it is vital to understand further the physiological mechanisms involved in the detoxification process following rGO exposure.

### Conflict of Interests

Authors declare no conflict of interests to disclose.

### Ethical approval

There were no animal ethical issues involved in carrying out this research.

### References

1. Meyer JC, Geim AK, Katsnelson MI *et al.* The Structure of Suspended Graphene Sheets. *Nature*,2007;446:60-3.
2. Compton OC, Nguyen ST. Graphene oxide, highly reduced graphene oxide, and graphene: versatile building blocks for carbon-based materials. *Small*,2010;6:711-23.
3. Zhou O, Shimoda H, Gao B *et al.* Materials science of carbon nanotubes: fabrication, integration and properties of macroscopic structures of carbon nanotubes. *Acc Chem Res*,2002;35:1045-53.
4. Xu Y, Wang Y, Liang J *et al.* A hybrid material of graphene and poly (3,4-ethyldioxythiophene) with high conductivity, flexibility, and transparency. *Nano Res*,2009;2:343-8.
5. Guldi DM, Rahman A, Sgobba V *et al.* Multifunctional molecular carbon materials-from fullerenes to carbon nanotubes. *Chem Soc Rev*,2006;35:471-87.
6. Kunzmann A, Anderson B, Thurnherr T *et al.* Toxicology of engineered nanomaterials: Focus on biocompatibility, biodistribution and biodegradation. *Biochim Biophys Acta*,2011;1810:361-73.
7. Kundu N, Yadav S, Pundir CS. Preparation and characterization of glucose oxidase nanoparticles and their application in dissolved oxygen metric determination of serum glucose. *J Nanosci Nanotechnol*,2013;13:1710-6.
8. Pumera M. Nanotoxicology: the molecular science point of view. *Chem Asian J*,2011;6:340-8.
9. Aruoja V, Dubourguier HC, Kasemets K *et al.* Toxicity of nanoparticles of CuO, ZnO and TiO<sub>2</sub> to microalgae *Pseudokirchneriella subcapitata*. *Sci Total Environ*,2009;407:1461-8.
10. Wang L, Nagesha DK, Selvarash S *et al.* Toxicity of CdSe nanoparticles in Caco-2 cell cultures. *J Nanobiotechnol*,2008;6:11-26.
11. Zhang XQ, Yin LH, Tang M *et al.* ZnO, TiO<sub>2</sub>, SiO<sub>2</sub>, and Al<sub>2</sub>O<sub>3</sub> nanoparticles-induced toxic effects on human fetal lung fibroblasts. *Biomed Environ Sci*,2011;24:661-9.
12. Tourinho PS, Gestel CAM, Lofts S *et al.* Critical review-metal-based nanoparticles in soil: fate, behavior and effects on soil invertebrates. *Environ Toxicol Chem*,2012;31:1679-92.
13. Lansiedel R, Hock LM, Kroll A *et al.* Testing metal-oxide nanomaterials for human safety. *Adv Mater*,2010;22:2601-27.
14. Zhu Y, Li W, Li Q *et al.* Effects of serum proteins on intracellular uptake and cytotoxicity of carbon nanoparticles. *Carbon*,2009;47:1351-8.
15. Zhang X, Yin J, Peng C *et al.* Distribution and biocompatibility studies of graphene oxide in mice after intravenous administration. *Carbon*,2011;49:986-95.
16. Zhang X, Hu W, Li J *et al.* A comparative study of cellular uptake and cytotoxicity of multi-walled carbon nanotubes, graphene oxide, and nano diamond. *Toxicol Res*,2012;1:62-8.
17. Zhang X, Yin J, Kang C *et al.* Biodistribution and toxicity of nano diamonds in mice after intratracheal instillation. *Toxicol Lett*,2010;198:37-43.
18. Zhang X, Zhu Y, Li J *et al.* Tuning the cellular uptake and cytotoxicity of carbon nanotubes by surface hydroxylation. *J Nanopart Res*,2011;12:6941-52.

19. Chen B, Song WM, Hayashi Y *et al.* *In Vitro* Evaluation of Cytotoxicity and Oxidative Stress Induced by Multiwalled Carbon Nanotubes in Murine RAW 264.7 Macrophages and Human A549 Lung Cell. *Biomed Environ Sci*,2011;24:593-601.
20. Chang Y, Yang ST, Liu JH *et al.* *In vitro* toxicity evaluation of graphene oxide on A549 cells. *Toxicol Lett*,2011;200:201-10.
21. Zhu X, Zhu L, Li Y *et al.* Developmental toxicity in zebrafish (*Danio Rerio*) embryos after exposure to manufactured nanomaterials: buckminsterfullerene aggregates (nC<sub>60</sub>) and fullerol. *Environ Toxicol Chem*,2007;26:976-9.
22. Zhang Y, Syed FA, Enkeleda D *et al.* Cytotoxicity effects of graphene and single-wall carbon nanotubes in neural phaeochromocytoma-derived pc12 cells. *ACS Nano*,2010;4:3181-6.
23. Yan L, Wang Y, Xu X *et al.* Can graphene oxide cause damage to eyesight? *Chem Res Toxicol*,2012;25:1265-70. 24.
24. Akhavan O, Ghaderi E. Toxicity of graphene and graphene oxide nanowalls against bacteria. *ACS Nano*,2010;4:57316.
25. OECD. Guideline for testing of chemicals, fish, acute toxicity test 203, 1992. OECD Publishing, <http://www.oecd.org/chemicalsafety/risk-assessment/1948241.pdf>
26. Barbazuk WB, Korf I, Kadavi C *et al.* The syntenic relationship of the zebrafish and human genomes. *Genome Res*,2000;10:1351-1358. <https://doi.org/10.1101/gr.144700>.
27. Souza JP, Baretta JF, Santos F, Paino IMM, Zucolotto V. Toxicological effects of graphene oxide on adult zebrafish (*Danio rerio*). *Aquat Toxicol*,2017;186:11-18. <https://doi.org/10.1016/j.aquatox.2017.02.017>.
28. Chen M, Yin J, Liang Y, Yuan S, Wang F, Song M *et al.* Oxidative stress and immunotoxicity induced by graphene oxide in zebrafish. *Aquat Toxicol*,2016b;174:54-60. <https://doi.org/10.1016/j.aquatox.2016.02.015>.
29. Fachini-Queiroz FC, Kummer R, Estevão-Silva CF, Carvalho MD, Cunha JM *et al.* Effects of thymol and carvacrol, constituents of *Thymus vulgaris* L. essential oil, on the inflammatory response. *Evidence-Based Complementary and Alternative Medicine*, 2012, 657026.
30. Fan K, Li X, Cao Y, Qi H, Li L, Zhang Q *et al.* Carvacrol inhibits proliferation and induces apoptosis in human colon cancer cells. *Anti-Cancer Drugs*,2015;26(8):813-823.
31. Fitsiou E, Anastopoulos I, Chlichlia K, Galanis A, Kourkoutas I, Panayiotidis M *et al.* Antioxidant and antiproliferative properties of the essential oils of *Satureja thymbra* and *Satureja parnassica* and their major constituents. *Anticancer Research*,2016;36(11):5757-5763.
32. Finkel T, Holbrook NJ. Oxidants, oxidative stress and the biology of ageing. *Nature*,2016;408(6809):239-247.
33. Fossella FV, DeVore R, Kerr RN, Crawford J, Natale RR, Dunphy F. the TAX Non-Small-Cell Lung Cancer Study Group. Randomized phase III trial of docetaxel versus vinorelbine or ifosfamide in patients with advanced non-small-cell lung cancer previously treated with platinum-containing chemotherapy regimens. *Journal of Clinical Oncology*,2000;18(12):2354-2362.
34. Giannenas I, Triantafyllou E, Stavrakakis S, Margaroni M, Mavridis S, Steiner T *et al.* Assessment of dietary supplementation with carvacrol or thymol containing feed additives on performance, intestinal microbiota and antioxidant status of rainbow trout (*Oncorhynchus mykiss*). *Aquaculture*,2012;350:26-32.
35. Harvey AL, Edrada-Ebel R, Quinn RJ. The re-emergence of natural products for drug discovery in the genomics era. *Nature Reviews. Drug Discovery*,2015;14(2):111-129.
36. Hashemipour H, Kermanshahi H, Golian A, Khaksar V. Effects of carboxy methyl cellulose and thymol+ carvacrol on performance, digesta viscosity and some blood metabolites of broilers. *Journal of Animal Physiology and Animal Nutrition*,2014;98(4):672-679.
37. Hashemipour H, Kermanshahi H, Golian A, Veldkamp T. Effect of thymol and carvacrol feed supplementation on performance, antioxidant enzyme activities, fatty acid composition, digestive enzyme activities, and immune response in broiler chickens. *Poultry Science*,2013;92(8):2059-2069.
38. He L, Mo H, Hadisusilo S, Qureshi AA, Elson CE. Isoprenoids suppress the growth of murine B16 melanomas *in vitro* and *in vivo*. *The Journal of Nutrition*,1997;127(5):668-674.
39. Jayakumar S, Madankumar A, Asokkumar S, Raghunandhakumar S, Gokula dhas K, Kamaraj S *et al.* Potential preventive effect of carvacrol against diethylnitrosamine-induced hepatocellular carcinoma in rats. *Molecular and Cellular Biochemistry*,2012;360(1-2):51-60.
40. Klein AH, Carstens MI, Carstens E. Eugenol and carvacrol induce temporally desensitizing patterns of oral irritation and enhance innocuous warmth and noxious heat sensation on the tongue. *Pain*,2013;154(10):2078-2087.
41. Zeytinoglu M. Effects of carvacrol on a human non-small cell lung cancer (NSCLC) cell line, A549. *Cytotechnology*,2003;43(1-3):149-154.
42. Karatzas AK, Kets EP, Smid EJ, Bennik MH. The combined action of carvacrol and high hydrostatic pressure on *Listeria monocytogenes* Scott A. *Journal of Applied Microbiology*,2001;90(3):463-469.
43. Rao JV. Sublethal effects of an organophosphorus insecticide (RPR-II) on biochemical parameters of tilapia, *Oreochromis mossambicus*. *Comp. Biochem. Physiol., Part C: Toxicol. Pharmacol*,2006;143(4):492-498. <https://doi.org/10.1016/j.cbpc.2006.05.001>.
44. Kavitha P, Rao JV. Oxidative stress and locomotor behaviour response as biomarkers for assessing recovery status of mosquito fish, *Gambusia affinis* after lethal effect of an organophosphate pesticide, monocrotophos. *Pestic. Biochem. Physiol*,2007;87(2):182-188. <https://doi.org/10.1016/j.pestbp.2006.07.008>.
45. Cao N, Zhang Y. Study of Reduced Graphene Oxide Preparation by Hummers: Method and Related Characterization. *J. Nanomater*, 2015, 5.
46. Ghafari Farsani H, Doria HB, Jamali H, Hasanpour S, Mehdipour N, Rashidiyan G. The protective role of vitamin E on *Oreochromis niloticus* exposed to ZnO NPs. *Ecotoxicol. Environ. Saf*,2017;145:1-7. <https://doi.org/10.1016/j.ecoenv.2017.07.005>.

47. Parry RM, Chandan RC, Shahani KM. A rapid and sensitive assay of muramidase. *Proc. Soc. Exp. Biol. Med*,1965;119(2):384-386.  
<https://doi.org/10.3181/00379727-119-30188>.
48. Aebi H. Catalase *in vitro*. *Methods Enzymol*,1984;105:121-126.  
[https://doi.org/10.1016/S0076-6879\(84\)05016-3](https://doi.org/10.1016/S0076-6879(84)05016-3).
49. Peyghan R, Takamy GA. Histopathological, serum enzyme, cholesterol and urea changes in experimental acute toxicity of ammonia in common carp *Cyprinus carpio* and use of natural zeolite for prevention. *Aquac. Int*,2002;10(4):L317-325.  
<https://doi.org/10.1023/A:1022408529458>.
50. Shaluei F, Hedayati A, Jahanbakhshi A, Baghfalaki M. Physiological responses of great sturgeon (*Huso huso*) to different concentrations of 2-phenoxyethanol as an anesthetic. *Fish Physiol. Biochem*,2012;38(6):1627-1634. <https://doi.org/10.1007/s10695-012-9659-4>.
51. Bradford M. A rapid sensitive method for the quantitation of microgram quantities of protein utilizing the principle of protein-dye binding. *Anal. Biochem*,1976;72(1-2):248-254.  
[https://doi.org/10.1016/0003-2697\(76\)90527-3](https://doi.org/10.1016/0003-2697(76)90527-3).
52. Bayunova L, Barannikova I, Semenkova T. Sturgeon stress reactions in aquaculture. *J. Appl. Ichthyol*,2002;18(4-6):397-404.  
<https://doi.org/10.1046/j.1439-0426.2002.00410.x>
53. Akhbari K, Morsali A, Mahmoudi G, Aslani A, Rafiei S, Chae HK *et al*. 66-Title: thallium(I) one-dimensional coordination polymer containing large tetranuclear metallacycle, [Tl<sub>2</sub> (μ-Htdp)<sub>2</sub> (μ-H<sub>2</sub>O)]<sub>n</sub> (H<sub>2</sub>tdp = 4,4'-thiodiphenol): thermal. fluorescence and structural studies, 2007, 463-475.
54. Balandin AA, Ghosh S, Bao W, Calizo I, Teweldebrhan D, Miao F *et al*. Superior thermal conductivity of single-layer graphene. *Nano Lett*,2008;8:902
55. Chen JH, Jang C, Ishigami M, Xiao S, Cullen WG, Williams ED *et al*. Diffusive charge transport in graphene on SiO<sub>2</sub>. *Solid State Commun*,2009;149:1080-1086.
56. Lee DY, Khatun Z, Lee JH, Lee YK, In I. Blood compatible graphene/heparin conjugate through noncovalent chemistry. *Biomacromolecules*,2011;12:336-341.
57. Kori-Siakpere O, Ikomi RB, Ogbe MG. Variations in acid phosphatase and alkaline phosphatase activities in the plasma of the African catfish: *Clarias gariepinus* exposed to sublethal concentrations of potassium permanganate. *Asian J. Exp. Biol. Sci*,2012;1(1):170-174.
58. Velisek J, Svobodova Z, Machova J. Effects of bifenthrin on some haematological, biochemical and histopathological parameters of common carp (*Cyprinus carpio* L.). *Fish Physiol. Biochem*,2009;35(4):583-590.  
<https://doi.org/10.1007/s10695-008-9258-6>.
59. Atli G, Ariyurek SY, Kanak EG, Canli M. Alterations in the serum biomarkers belonging to different metabolic systems of fish (*Oreochromis niloticus*) after Cd and Pb exposures. *Environ. Toxicol. Pharmacol*,2015;40(2):508-515.  
<https://doi.org/10.1016/j.etap.2015.08.001>.
60. Sulaiman FA, Adeyemi OS, Akanji MA, Oloyede HOB, Sulaiman AA, Olatunde *et al*. Biochemical and morphological alterations caused by silver nanoparticles in Wistar rats. *J. Acute Med*,2015;5(4):96-102.  
<https://doi.org/10.1016/j.jacme.2015.09.005>.